

Temperature and pressure dependence of the rain-snow phase transition over land and ocean

Aiguo Dai¹

Received 14 January 2008; revised 26 March 2008; accepted 29 April 2008; published 17 June 2008.

[1] The phase of precipitation is important for weather forecasts, land hydrology and remote sensing. To quantify the temperature and pressure dependence of snow frequency (F , in %) when precipitation occurs, we have analyzed 3-hourly weather reports of surface air temperature (T_s , °C) and pressure (P_s), and snow and rain occurrences from over 15,000 land stations and available ship observations from 1977–2007. It is found that the phase transition occurs over a fairly wide range of temperature from about -2°C to $+4^{\circ}\text{C}$ over (low-elevation) land and -3°C to $+6^{\circ}\text{C}$ over ocean. The F - T_s relationship can be represented by a hyperbolic tangent: $F(T_s) = a [\tanh(b(T_s - c)) - d]$, with the slope parameter b close to 0.7 over land and 0.4 over ocean. The pressure-dependence is only secondary and reflected in the parameters. Results show that snow occurs often ($F > 50\%$) for $T_s \leq 1.2^{\circ}\text{C}$ over land and $T_s \leq 1.9^{\circ}\text{C}$ over ocean, and are non-negligible ($F > 5\%$) for $T_s \leq 3.8^{\circ}\text{C}$ over land and $T_s \leq 5.5^{\circ}\text{C}$ over ocean. This “warm bias” results from the falling of snowflakes into warmer surface layers, which is especially true over ocean. The warm bias is higher when air pressure is below ~ 750 hPa because snow falls faster in thin air.

Citation: Dai, A. (2008), Temperature and pressure dependence of the rain-snow phase transition over land and ocean, *Geophys. Res. Lett.*, 35, L12802, doi:10.1029/2008GL033295.

1. Introduction

[2] Snow can accumulate on the ground and increase surface albedo; whereas rain often increases soil moisture and evaporation, or results in runoff. Thus, snow and rain have very different effects on land hydrology and the climate [Slater *et al.*, 2001], and a realistic representation of the phase of precipitation in weather and climate models is highly desirable. Most current models, however, use simple temperature-dependence to calculate the fraction of snowfall. For example, in the Community Atmospheric Model Version 3.0 (CAM3.0) [Collins *et al.*, 2004] precipitation production is 100% snow when the air temperature is less than -5°C and this fraction linearly decreases to zero at 0°C . As shown previously [e.g., Auer, 1974], snowfall can occur at temperatures well above 0°C . Most current climate models, however, overestimate snowfall amount in winter and spring [Roesch, 2006]. In addition to modeling snowfall, the phase of precipitation is also important for ground-based radar [Ryzhkov and Zrnicek, 1998] and satellite [Noh *et al.*, 2006] remote sensing of precipitation, because snow flakes and rain droplets have different radiative properties.

[3] Although water normally freezes at 0°C , the freezing point can change when it contains other substances, as in rain droplets and seawater. The rain-snow phase transition near the surface is further complicated by other factors: (1) snowflakes and rain droplets fall through the lower troposphere where temperature usually increases toward the surface; (2) snowflakes take a finite time to melt, which allows falling snow to exist in warm layers; and (3) this “warm bias” varies with the fall speed (a function of air pressure and particle size [Yuter *et al.*, 2006]) of snowflakes and atmospheric lapse rates. Since it is impractical to simulate all these aspects in numerical models, one may use the empirical temperature and pressure dependence of snow frequency observed at the surface to parameterize the phase transition.

[4] There have been a relatively few studies on the dependence of precipitation phase on temperature and other factors. Analyses of limited station data from England [Murray, 1952] and the U.S. [U.S. Army Corps of Engineers, 1956] show that precipitation occurs as snow nearly 100% of the time when surface air temperature (T_s) is below about -1°C . This frequency decreases slowly as T_s increases to 0°C and then declines rapidly to $\sim 20\%$ at 2°C . Analyses of ~ 1000 samples from U.S. stations by Auer [1974] revealed similar rain-snow phase transition. Based on these analyses, a simple, stepwise rain-snow transition is often used in hydrological and land surface modeling with a critical T_s between 1.7 – 2.5°C [U.S. Army Corps of Engineers, 1956; Yang *et al.*, 1997].

[5] To help model parameterization and remote sensing of snow and rainfall, here we analyze over 30 years of synoptic weather reports from land stations and ships over the globe to quantify the temperature- and pressure-dependence of the rain-snow phase transition over both land and ocean. The results are then fitted with analytic nonlinear functions so that they can be used in numerical modeling and remote sensing.

2. Data and Methods

[6] We used the 3-hourly synoptic weather reports, which include, among others, near-surface (around 1.5 – 2.0 m above the ground) air temperature (T_s) and pressure (P_s), and the occurrence of various types of precipitation at or near the observation location and at the time of observation or during the preceding hour. There are over 15,000 land stations and many ships around the globe that routinely make these weather reports, which are archived at the National Center for Atmospheric Research (<http://dss.ucar.edu/datasets/ds464.0/>) and have been used by the author to quantify the occurrence frequency of various precipitation types [Dai, 2001a] and their diurnal variations [Dai, 2001b],

¹National Center for Atmospheric Research, Boulder, Colorado, USA.

as well as other applications [e.g., Dai, 2006]. Here we used the data from manned stations or ships only and from January 1977 to February 2007, which provides a very large number of samples (see Dai [2001a, 2006] for geographic distributions of the samples). In the weather reports a unique code is used to indicate the occurrence of various weather events, such as snow, rain, or sleet (i.e., mixture of snow and rain). Here snow events include any reports of snow, freezing rain, or freezing drizzles (present weather code ww = 22, 24, 26, 56–57, 66–67, 70–79, 85–86, 93–94; see [Dai, 2001a] for the meaning of the codes), rain events include all the cases of liquid precipitation (including drizzles, ww = 20–21, 25, 27, 29, 50–55, 58–65, 80–82, 88–99), and sleet events include any reports of mixed rain and snow at the same time (ww = 23, 68–69, 83–84, 87). Tests showed that inclusion of drizzles had only minor effects and inclusion of sleet reduces the snow and rain frequency slightly.

[7] The snow, rain and sleet reports from all manned stations or ships were counted together for each 0.25°C T_s bin between -10°C and 10°C to quantify the temperature dependence. The number of precipitation events (for all

seasons combined) for each 0.25°C bin ranges from $\sim 100,000$ to over 1 million over land and a few thousands to over 50 thousands over ocean. They were also counted for each bin of 0.25°C of T_s and 50 hPa of P_s for quantifying both the temperature and pressure dependence. These counts were converted into percentages of frequency (F) by dividing the counts with the total counts of precipitation events. The frequency is referred to as conditional snow, rain, or sleet frequency, which may be interpreted as the probability of snow, rain, or sleet when precipitation occurs. The counting was done for each season and all-season combined.

[8] We found that the F (%) – T_s ($^{\circ}\text{C}$) relationship for snow and rain can be well fitted with a hyperbolic tangent function like this:

$$F(T_s) = a[\tanh(b(T_s - c)) - d] \quad (1)$$

where a , b , c , and d are parameters estimated using the Levenberg-Marquardt method for nonlinear least squares fitting [Press *et al.*, 1992]. The F 's dependence on air pressure was found to be only secondary and was accounted

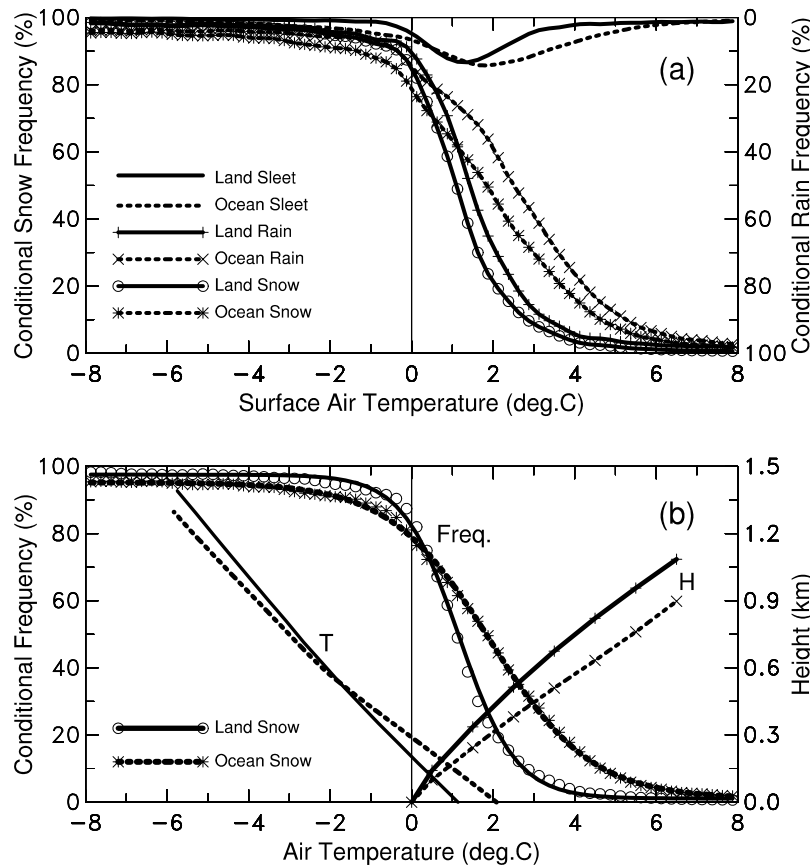


Figure 1. (a) Observed temperature-dependence of the conditional snow, rain, and sleet frequency (read on the right ordinate) during all seasons from 1977–2007 over global land (solid line) and ocean (dashed line). (b) The snow frequency over land (circles) and ocean (stars) from Figure 1a overlaid by the fitted frequency (lines) using equation (1). Also shown in Figure 1b is the mean temperature profiles (denoted by “T”, right ordinate, which is the height above the surface) derived from the 6-hourly ERA-40 reanalysis [Uppala *et al.*, 2005] from 1980–1989 by averaging over the land (solid line, slope = $-5.1^{\circ}\text{C km}^{-1}$ for the lowest 1 km) and ocean (dashed line, slope = $-6.6^{\circ}\text{C km}^{-1}$) areas where surface air temperature (T_s) is within the snow-rain transition range (-2°C to 4°C for land and -3°C to $+6^{\circ}\text{C}$ for ocean). The mean height of the freezing level as a function of T_s is also shown (denoted by “H”, solid line = land, dashed = ocean).

Table 1a. Least-Squares Estimates of the Parameters in the Hyperbolic Tangent $F(T_s) = a [\tanh(b(T_s - c)) - d]$ for Annual and Seasonal Snow Frequency When Precipitation Occurs as a Function of Surface Air Temperature^a

Case	a	b	c	d	χ^2
Land, ANN	-48.2292	0.7205	1.1662	1.0223	71.01
Ocean, ANN	-47.1472	0.4049	1.9280	1.0203	7.82
Land, DJF	-48.2372	0.7449	1.0919	1.0209	84.05
Ocean, DJF	-47.1823	0.4003	2.1735	1.0255	6.08
Land, MAM	-48.2493	0.6634	1.3388	1.0270	78.01
Ocean, MAM	-47.0035	0.4090	1.7372	1.0226	14.27
Land, JJA	-46.4000	0.7013	0.8362	1.0217	142.87
Land, SON	-48.3251	0.7798	1.1502	1.0180	50.97
Ocean, SON	-46.8494	0.4162	2.0474	1.0155	13.22

^aFrequency: F , in %; surface air temperature: T_s , in °C. The sum of the cumulative error (χ^2) is also shown (a smaller value indicates a better fit). Drizzles were included in this calculation. Note that the frequency (%) for sleet (mixture of snow and rain) is $100 - (\text{snow} + \text{rain})$ frequency.

for by allowing the parameters to be functions of pressure. In all F - T_s plots shown below, an 11-point digital filter was used to slightly smooth (but keep the shape of) the curves, and the fitting was done on the smoothed curves.

3. Results

[9] Figure 1a shows the T_s -dependence of the annual-mean conditional snow, rain and sleet frequency (F) over land (solid line) and ocean (dashed line). When precipitation occurs over land, snow is observed over 95% of the time when $T_s \leq -2.0^\circ\text{C}$. This frequency (solid line with open circles in Figure 1a) slowly decreases as T_s increases to 0°C , after that it declines rapidly to below 5% for $T_s \geq 3.7^\circ\text{C}$ and essentially zero (<1%) above 6.5°C . Over the oceans, the drop in the snow frequency (dashed line with asterisk in Figure 1a) for $T_s > 0^\circ\text{C}$ is slower than that over land, resulting in considerable snow occurrence (>5%) for T_s up to 5.5°C . The rain frequency, shown on the right-hand-side ordinate of Figure 1a, is almost the opposite of the snow frequency, with a slight downward shift (decrease) of the frequency to account for the small sleet frequency (lines without symbols in Figure 1a), which roughly follows a normal distribution with a peak of $\sim 13.3\%$ around 1.4°C over land and $\sim 14.3\%$ near 1.9°C over ocean. We notice that the 50% frequency for both snow and rain occurs at temperatures (referred to as half-frequency temperature or $T_{0.5}$) considerably above 0°C , around 1.2°C for land snow and 1.9°C for ocean snow (see the “ c ” parameter in

Tables 1a and 1b). This “warm bias” mainly results from the fact that snowflakes take a finite amount of time (~ 10 minutes according to *U.S. Army Corps of Engineers* [1956]) to melt during which they fall into warmer air layers near the surface. The higher $T_{0.5}$ over ocean than land is primarily due to the larger temperature gradient over ocean surface ($-6.6^\circ\text{C km}^{-1}$) than over land surface ($-5.1^\circ\text{C km}^{-1}$) during the cold season, which means lower freezing levels for a given T_s over ocean (Figure 1b). For these lapse rates, the corresponding freezing level for $T_s = T_{0.5}$ is 229 m over land and 292 m over ocean, which are consistent with *Murray* [1952], who found that snow dominates when the freezing level is below 900 feet (274 m) while rain dominates when the freezing level is above 1000 feet (305 m).

[10] Our frequencies for snow, rain and sleet over land are generally consistent with those reported by *Murray* [1952] and *U.S. Army Corps of Engineers* [1956] (see the insert in Figure 2a), although our results show slightly lower snow (higher rain) frequency for $T_s < 0^\circ\text{C}$ and higher snow (lower rain) frequency for $T_s > +3^\circ\text{C}$. Given the small probability at these temperatures and the limited sample sizes (<2500) in the earlier studies, it is likely that their occurrence frequencies contain large uncertainties near the two ends of the transition zone.

[11] Another asymmetric feature in Figure 1a is that the snow frequency at cold temperatures ($< -3^\circ\text{C}$) approaches 100% at a pace slower than that for the rain frequency to converge to 100% at warm temperatures ($> 6^\circ\text{C}$). This is especially true over ocean and it may result from the effect

Table 1b. Least-Squares Estimates of the Parameters in the Hyperbolic Tangent $F(T_s) = a [\tanh(b(T_s - c)) - d]$ for Annual and Seasonal Rain Frequency When Precipitation Occurs as a Function of Surface Air Temperature^a

Case	a	b	c	d	χ^2
Land, ANN	-47.8337	-0.6866	1.4913	1.0420	62.14
Ocean, ANN	-47.3041	-0.4263	2.5687	1.0784	6.05
Land, DJF	-47.5770	-0.6856	1.3942	1.0438	76.00
Ocean, DJF	-47.0262	-0.4360	2.8572	1.0731	4.70
Land, MAM	-47.9077	-0.6603	1.6927	1.0358	75.31
Ocean, MAM	-47.2828	-0.4299	2.3397	1.0800	9.36
Land, JJA	-46.8303	-0.6595	1.1582	1.1056	101.75
Land, SON	-48.0315	-0.7663	1.4640	1.0412	40.29
Ocean, SON	-47.2107	-0.4280	2.7118	1.0911	14.19

^aFrequency: F , in %; surface air temperature: T_s , in °C. The sum of the cumulative error (χ^2) is also shown (a smaller value indicates a better fit). Drizzles were included in this calculation. Note that the frequency (%) for sleet (mixture of snow and rain) is $100 - (\text{snow} + \text{rain})$ frequency.

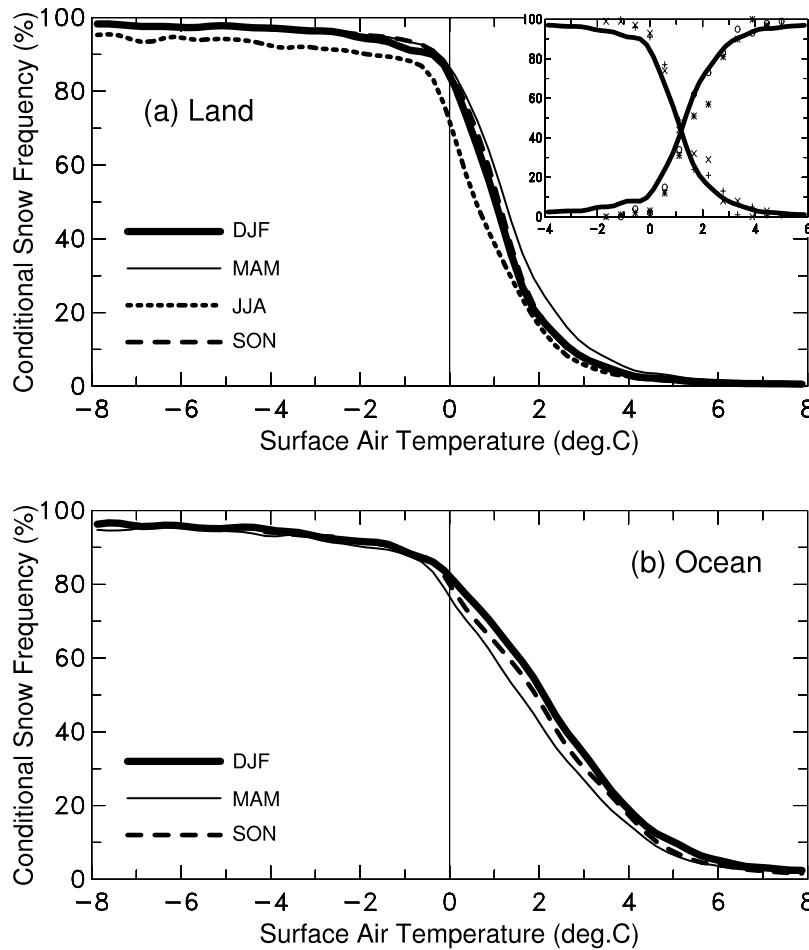


Figure 2. Observed temperature-dependence of the seasonal conditional snow frequency (%) over (a) land and (b) ocean (data for JJA are insufficient). The insert inside Figure 2a compares the snow and rain DJF frequency from this study (lines) with those (symbols) from Murray [1952] and U.S. Army Corps of Engineers [1956].

of salt in cloud droplets that can lower the freezing point. At the same time, liquid rain is seldom observed ($F < 5\%$) at temperatures just a few $^{\circ}\text{C}$ below zero, in contrast to supercooled cloud water that can exist at temperatures well below 0°C [Naud *et al.*, 2006].

[12] The F - T_s relationship for both snow and rain can be reasonably represented by a (transformed) hyperbolic tangent function (equation (1)). Figure 1b compares the fitted lines with the data points used in Figure 1a for snow frequency over land and ocean. The estimated parameters are shown in Tables 1a and 1b, together with χ^2 , the sum of the (normalized) differences between the observed and estimated F . Parameter a is a scaling factor, b is the slope (scaled by a) around $T_{0.5}$, c approximately represents the half-frequency temperature $T_{0.5}$ in $^{\circ}\text{C}$, and d , when different from one, reflects the slight asymmetry in the converged values at large negative and positive temperatures. Not surprisingly, the largest discrepancy occurs around the curving parts of the lines, with oceanic snow frequency fitted better (Figure 1b).

[13] The seasonal F - T_s relationship for snow is shown in Figure 2, except for JJA over (mainly southern) oceans where sampling is insufficient. Over land, the seasonal differences are small, except for JJA when snow occurs at relatively few locations north of 60°N , around the southern

tip of South America, and over the Tibetan Plateau [Dai, 2001a]. Since the JJA snow events occur mostly around the high-latitude coastal areas, cloud droplets may contain high concentrations of sea salt (from maritime aerosols [see Jaenickle, 1993]) which can lower the freezing point. This may partly explain the relatively low snow but high rain frequency for JJA (Figure 2a) for $T_s < 1.5^{\circ}\text{C}$.

[14] The oceanic seasonal F - T_s relationship for snow (Figure 2b) follows the annual slope ($b = 0.40$ – 0.42 , compared with 0.66 – 0.78 over land; see Table 1a) and shows higher snow (lower rain) frequency than over land from about $+0.5^{\circ}\text{C}$ to 6°C . The seasonal differences are small, although during boreal spring (March–May or MAM) the snow frequency is slightly lower over the phase transition temperature range. Table 1a shows that parameter c (a proxy of the half frequency temperature $T_{0.5}$) is consistently larger over ocean (1.7 – 2.2) than over land (0.8 – 1.3) for all seasons, confirming the effect of a warm ocean surface that induces a large vertical temperature gradient in the air.

[15] To explore the additional pressure-dependence of the snow frequency over land, we stratified the station weather reports for each 50 hPa pressure and 0.25°C temperature bin at the same time, and the results (after some smoothing) are plotted in Figure 3a. The F - T_s relationships at two selected

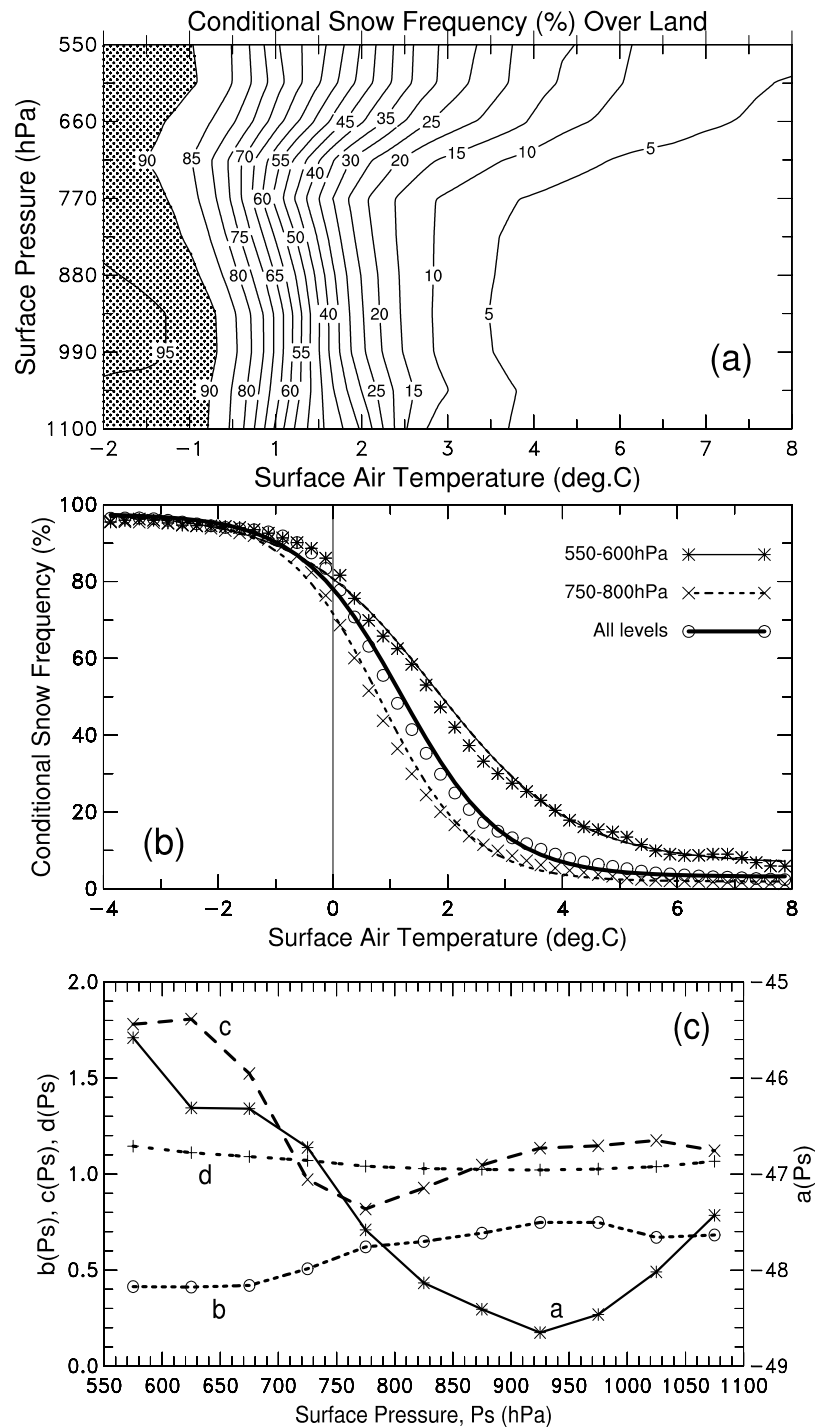


Figure 3. (a) Observed conditional snow frequency (%) over land as a function of station air temperature and pressure. (b) Observed (symbols) and fitted (lines) temperature-dependence of the conditional snow frequency (%) for 550–600 hPa, 750–800 hPa, and averaged over all pressure levels in Figure 3a. (c) The pressure-dependence of the estimated parameters a , b , c and d of equation (1).

levels and averaged over all levels are shown in Figure 3b, and the estimated parameters of equation (1) are plotted in Figure 3c as a function of station pressure. From the sea level to about 750 hPa, pressure's effect is very small, as shown by Figure 3a and the relatively small variations in the estimated parameters (Figure 3c). Above 750 hPa, however, pressure's effect is evident, with $T_{0.5}$ (see c in Figure 3c)

increasing from $\sim 1.0^\circ\text{C}$ to 1.8°C and the slope (b in Figure 3c) decreasing from ~ 0.7 to 0.4 . The scaling factor a is also lower (i.e., larger negative values) at higher pressures. The overall effect is a more ocean-like F - T_s relationship at high elevations ($P_s < 700$ hPa). Because the fall speed of raindrops and other hydrometeors decreases with air pressure (p) at a rate of $p^{-\alpha}$, where α is about 0.4 – 0.5 [Stull, 2000;

Del Genio et al., 2005], snowflakes fall faster in thin air and thus can reach higher temperatures near the surface before they melt. It is unclear, however, why this effect is not apparent at lower altitudes ($P_s > 750$ hPa).

4. Summary and Concluding Remarks

[16] We have analyzed over 30 years (1977–2007) of 3-hourly weather reports from global land stations and ship observations to quantify the temperature and pressure dependence of rain-snow phase transition near the surface. The analysis focused on the differences between land and ocean and between low- and high-elevation areas. It is found that the phase transition occurs over a fairly wide range of surface air temperature from about -2°C to $+4^{\circ}\text{C}$ over (low- to moderate-elevation) land and -3°C to $+6^{\circ}\text{C}$ over ocean. The observed snow (including freezing rain) occurrence frequency (F , i.e., the probability for snowing) when precipitation occurs follows a hyperbolic tangent function of surface air temperature (T_s), so that the half-frequency occurs around 1.2°C over land and 1.9°C over ocean (instead of at 0°C) with a dF/dT_s slope (before scaling by parameter a in equation (1)) of 0.72 over land and 0.40 over ocean at the half-frequency temperature ($T_{0.5}$). This “warm bias” in $T_{0.5}$ mainly results from the falling of snowflakes into warmer air layers over the surface, and the land-ocean differences in $T_{0.5}$ and the slope are due to the larger vertical temperature gradients over warm ocean surfaces in the cold season. Seasonal differences in the F - T_s relationship are small, although the snow frequency over land at high-latitudes and high terrain during JJA is slightly lower than during the other seasons. Significant pressure-dependence is found only at very high-elevations ($P_s < 750$ hPa), where snowflakes fall faster in thin air and thus can reach higher temperatures near the surface before melting. As a result, the F - T_s relationship at very high-elevations is similar to that over the oceans, with $T_{0.5}$ around 1.5 – 1.8°C and a slope around 0.4.

[17] The F - T_s relationship for rain is almost the opposite of that for snow, with a small shift toward higher T_s because of infrequent occurrence of sleet. Thus, the rain frequency can also be approximated by equation (1), with a negative slope b and a slightly larger $T_{0.5}$. The sleet frequency follows a normal distribution with a peak of $\sim 13.3\%$ around 1.4°C over land and $\sim 14.3\%$ near 1.9°C over ocean. The occurrence frequencies reported here are consistent with previous analyses of much smaller samples, although our results show slightly lower snow (higher rain) frequency for $T_s < 0^{\circ}\text{C}$ and higher snow (lower rain) frequency for $T_s > +3^{\circ}\text{C}$.

[18] The infrequent occurrence of sleet suggests that precipitation often occurs in single phase. Many climate models, however, often partition total precipitation into snow and rain at the same time when temperature is near the freezing point. A more realistic approach to apply the observed F - T_s relationship is to use a random number generator that has three outcomes (e.g., 1 for snow, 2 for rain, and 3 for sleet, whose snow and rain fractions are functions of T_s similar to equation (1)), whose probability functions at a given T_s follow the F - T_s relationships. This

will ensure the models have the observed mean phase dependence on T_s while allowing only one precipitation phase at most of the time. Besides the potential applications in modeling and remote sensing, our results can also be used to improve estimates of the potential changes in snowfall and rainfall under global warming.

[19] **Acknowledgments.** I thank two anonymous reviewers for helpful comments, Tony Del Genio and Kevin Trenberth for constructive discussions, Guosheng Liu for a conversation that partly motivated this study, Dick Valent and S. S. Ghosh for helpful discussions on non-linear fitting, and John Fasullo for help with the ERA-40 data. NCAR is sponsored by the National Science Foundation. This work was supported by NASA grant NNX07AD77G and NCAR's Water Cycle Program.

References

- Auer, A. H. (1974), The rain versus snow threshold temperatures, *Weatherwise*, 27, 67.
- Collins, W. D., et al. (2004). Description of the NCAR Community Atmosphere Model (CAM3), *Tech. Rep. NCAR/TN-464+STR*, 226 pp., Natl. Cent. for Atmos. Res., Boulder, Colo. (Available at <http://www.cesm.ucar.edu/models/atm-cam/docs/description/description.pdf>)
- Dai, A. (2001a), Global precipitation and thunderstorm frequencies. Part I: Seasonal and interannual variations, *J. Clim.*, 14, 1092–1111.
- Dai, A. (2001b), Global precipitation and thunderstorm frequencies. Part II: Diurnal variations, *J. Clim.*, 14, 1112–1128.
- Dai, A. (2006), Recent climatology, variability and trends in global surface humidity, *J. Clim.*, 19, 3589–3606.
- Del Genio, A. D., W. Kovari, M.-S. Yao, and J. Jonas (2005), Cumulus microphysics and climate sensitivity, *J. Clim.*, 18, 2376–2387.
- Jaenicke, R. (1993). Tropospheric aerosols, in *Aerosol-Cloud-Climate Interactions*, edited by P. V. Hobbs, pp. 1–32, Academic Press, San Diego, Calif.
- Murray, R. (1952), Rain and snow in relation to the 1000–700 mb and 1000–500 mb thicknesses and the freezing level, *Meteorol. Mag.*, 81, 5–8.
- Naud, C. M., A. D. Del Genio, and M. Bauer (2006), Observational constraints on the cloud thermodynamic phase in midlatitude storms, *J. Clim.*, 19, 5273–5288.
- Noh, Y. J., G. S. Liu, E. K. Seo, J. R. Wang, and K. Aonashi (2006), Development of a snowfall retrieval algorithm at high microwave frequencies, *J. Geophys. Res.*, 111, D22216, doi:10.1029/2005JD006826.
- Press, W. H., S. A. Teukolsky, W. T. Vetterling, and B. P. Flannery (1992). *Numerical Recipes in Fortran 77*, 2nd ed., 933 pp., Cambridge Univ. Press, Cambridge, UK.
- Roesch, A. (2006), Ion of surface albedo and snow cover in AR4 coupled climate models, *J. Geophys. Res.*, 111, D15111, doi:10.1029/2005JD006473.
- Ryzhkov, A. V., and D. S. Zrnic (1998), Discrimination between rain and snow with a polarimetric radar, *J. Appl. Meteorol.*, 37, 1228–1240.
- Slater, A. G., et al. (2001), The representation of snow in land surface schemes: Results from PILPS 2(d), *J. Hydrometeorol.*, 2, 7–25.
- Stull, R. (2000). *Meteorology for Scientists and Engineers*, 2nd ed., 502 pp., Brooks-Cole, Monterey, Calif.
- Uppala, S. M., et al. (2005), The ERA-40 re-analysis, *Q.J.R. Meteorol. Soc.*, 131, 2961–3012.
- U.S. Army Corps of Engineers (1956). Summary report of the snow investigation—Snow hydrology, North Pacific Division report, 437 pp., Washington, D. C. (Available at <http://www.crrel.usace.army.mil/icejams/Reports/1956%20Snow%20Hydrology%20Report.htm>)
- Yang, Z. L., R. E. Dickinson, A. Robock, and K. Y. Vinnikov (1997), Validation of the snow submodel of the biosphere-atmosphere transfer scheme with Russian snow cover and meteorological observational data, *J. Clim.*, 10, 353–373.
- Yuter, S. E., D. E. Kingsmill, L. B. Nance, and M. Löffler-Mang (2006), Observations of precipitation size and fall speed characteristics within coexisting rain and wet snow, *J. Appl. Meteorol. Climatol.*, 45, 1450–1464.

A. Dai, National Center for Atmospheric Research, P.O. Box 3000, Boulder, CO 80307-3000, USA. (adai@ucar.edu)